Lowland Technology International 2018; 20 (1): 15-26
International Association of Lowland Technology (IALT): ISSN 1344-9656

Research Paper

Full-scale Tests of Ground Anchors in Alluvium Soils of Egypt

M. F. Awad-Allah

ARTICLE INFORMATION

Article history:

Received: 01 October, 2017
Received in revised form: 17 January, 2018
Accepted: 19 January, 2018
Publish on: 01 June, 2018

Keywords:

Full-scale anchor
Alluvium soils
Anchorage
Skin friction resistance
Field test

ABSTRACT

This paper presents full-scale pullout ground anchor tests conducted in some types of alluvial soil formations in Egypt, including silty sand, sandstone, and clay soils. The tests were carried out up to failure loads in order to estimate the ultimate load of friction bearing capacity for each soil stratum. Moreover, an elaborated site investigation program was performed to predict the in-situ soil properties. This research campaign is a part of construction of residential and commercial complex which comprises six underground basements, and the site is located in a vital and highly traffic zone of Heliopolis, Cairo, Egypt. Field test setup and installation method of the full-scale ground anchors were explained. The results of the field tests were compared against the design values of unit skin friction resistance given by the well-known codes of practice (AASHTO; BS 8081; and Canadian Foundation Engineering Manual) and the literature for design of ground anchorage. The comparison showed that the values of skin friction resistance for anchor-soil/rock interface given in AASHTO (2004) and BS 8081 (1989) can be employed for determination of pullout capacities of ground anchors installed in Egyptian soils with a good reliability.

1. Introduction

Grouted ground anchor (**Fig. 1**) is a structural component used to transmit tension force from the structure to the subgrade, and it aims to provide a way to stabilize retaining works, either during the construction stage (temporary ground anchor) or along the entire life span of the retaining structure (permanent ground anchor). Moreover, ground anchors are typically used as a supports of retaining structures of excavations, for slopes stabilization, or against the uplift or overturning of structures.

In the literature, several theories have been proposed to predict the load bearing capacity of ground anchor, and the load transfer behavior of various types of ground anchors has been studied and reported by several researchers (e.g., Weerasinghe and Littlejohn; 1977, Benmokrane et al.; 1995, Barley; 1997a, 1997b, Jarrel and Haberfield; 1997, Woods and Barkhordari; 1979, Briaud et al.; 1998, and Kim; 2003). The significant influence of relative density, particle size distribution, and grouting pressure on the shear resistance along the bond length has been highlighted by Petrasovits (1981). Although the previous studies have shed light on the mechanism of the soil–anchor interaction, the load transfer mechanism of ground anchors needs to be investigated to better understand the behavior of ground anchors based on full scale pullout tests.

To date, there are no established Egyptian guidelines tailored for design, analysis, and construction of ground anchors. Because of scarcity of actual field data, the designers and contractors usually use the international well-known codes of practices for design of these structurers. Moreover, the Egyptian code (issue, 2005) does not address or deal with design and construction of ground anchor in detailed and very little guidance is given

Researcher, Ph.D., Civil Engineering Dept., National Research Center, EGYPT, mf.awad-alla@nrc.sci.eg
Note: Discussion on this paper is open until December 2018.

concerning that topic. Therefore, this paper presents the results of full scale pullout tests of ground anchors installed into the Egyptian soils including sandstone, silty sand, and clay. The measured ultimate soil-grout friction resistances were compared against the prescribed design values given in the international widely used codes of practice for ground anchorages (AASHTO, 2004; BS 8081, 1989; and Canadian Foundation Engineering Manual - CFEM, 2006).

Key:

1- Anchorage point at jack during stressing	7- Borehole	L_{fixxed}= Fixed anchor length
2- Anchorage point at anchor head in service	8- Debonding sleeve	L_{free} = Free anchor length
3- Plate bearing	9- Tendon	L_{tb} = Tendon bond length
4- Load transfer back	10- Grout body	L_{tf} = Tendon free length
5- Structure element	L_e= External length of tendon	
6- Soil/rock		

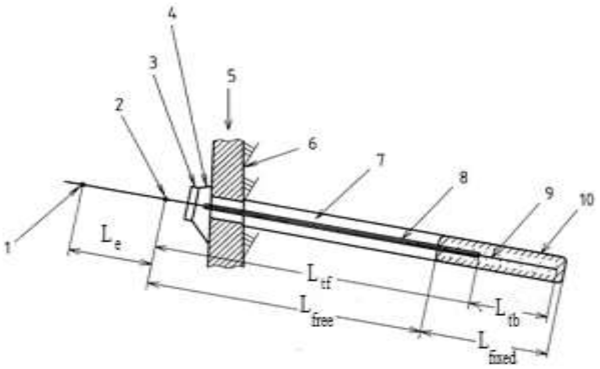

Fig. 1. Sketch of aground anchor (after EN-1537, 2000).

2. Anchor pullout capacity

2.1 General design formula

The ultimate pullout capacity of straight shaft ground anchors is determined by the friction load between the anchor grout and the soil (Q_{uf}), or the pullout load between the grout and the strand (Q_{up}), or the ultimate tensile load of strand (Q_{su}), whichever is smaller. Designs are normally based on the assumption of an equivalent uniform skin friction along the bond length.

The ultimate friction resistance Q_{uf} at the soil–grout interface can be calculated as follows:

$$Q_{uf} = \pi D L_{fixed} \tau_{ult} \qquad [1]$$

where: Q_{uf} is the ultimate friction; D is the diameter of anchor or effective diameter of borehole; L_{fixed} is the anchor-fixed (bonded) length of tension anchors or bonded transmission length of compression anchors, and τ_{ult} is the ultimate skin friction resistance between soil and grout which can be correlated to various soil properties and anchor types, as reported by PTI (1996).

The pullout force between grout and strand can be calculated as follows:

$$Q_{up} = \pi n d_e L_{tb} f_{ub} \qquad [2]$$

where: n is the number of strands; f_{ub} is the ultimate bond stress between grout and strand; L_{tb} is the bonded length of strand; and d_e is the effective diameter of strand.

The ultimate tensile load of strand Q_{us} can be calculated as follows:

$$Q_{us} = A_s f_{us} \qquad [3]$$

where: A_s is the cross-sectional area of strand, and f_{us} is the ultimate tensile stress of strand.

The ultimate compressive or shear resistance of grout Q_{ug} can be calculated as follows:

$$Q_{ug} = A_g f_{uc} \qquad [4]$$

where: f_{uc} is the ultimate compressive strength of grout or pure shear strength of grout, and A_g is the grout area or shear area. This criterion depends on the type of anchor body, either end bearing plate or tube type.

2.2 *Soil*-grout friction resistance proposed by codes of practice

Anchor pullout capacity is influenced by soil and rock conditions, method of anchor installation, hole diameter, bond length, grout type, and grouting pressure (Sabatini, et al. 1999; PTI, 1996; Cheney, 1984; and Weathersby, 1982). The design values of skin friction resistance given in the international codes of practice of ground anchors (e.g., AASHTO, 2004; BS 8081, 1989; and CFEM, 2006) are based on design curves or presumptive empirical values created from field experience in a range of soils rather than relying on a theoretical or empirical equation using the mechanical properties of a particular soil. Appendix (A) summarizes the design tables and design charts given in each code of practice for prediction of ultimate skin friction resistances (τ_{ult}) due to pullout force on ground anchors constructed in cohesionless soils, cohesive soils and rock.

2.3 *Evaluation* of ultimate pullout load

To estimate the ultimate load of an anchor from a pullout test that was not carried out to failure, many methods have been proposed in the literature to extrapolate the load-displacement curve. In this study, the method proposed by Chin (1970) was implemented, which is originally used for estimation of failure load of vertically loaded piles. This method, termed the Chin-Kondner, is based on the assumption that the relationship between the applied load (Q) and anchor displacement (S) is a hyperbolic relationship, and that a plot of (S/Q) versus (S) is linear. Consequently, a straight line can be obtained by plotting the measured anchor head displacements divided by the corresponding loads on the y-axis and the anchor head displacement on the x-axis, as shown in **Fig. 2**. In a typical anchor pullout test, the values will fall along a straight line after some initial variation. Eq. (5) represents a standard form of straight line equation for that line. The inverse of the slope of that equation, gives the ultimate failure load (Eq. 6).

$$S/Q = C_1 S + C_2 \quad [5]$$

$$(Q_u)_m = \frac{1}{C_1} \quad [6]$$

where: C_1 = slope of the straight line, C_2 = intercept of the S/Q axis.

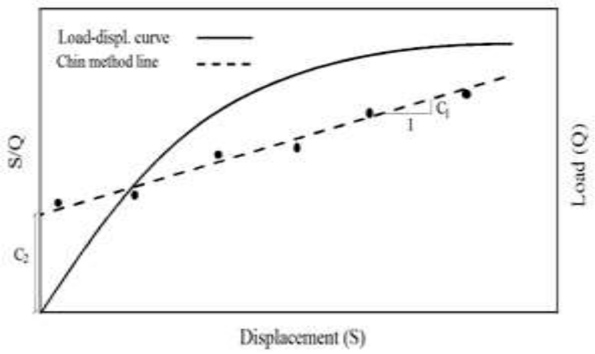

Fig. 2. Prediction of ultimate failure load using Chin-Kondner criterion (after Chin 1970).

3. General description of the project and the site

3.1 Project and site conditions

The proposed site is located in Nozha Street, Heliopolis, Cairo, and the project to be constructed on a built up area of 35186 m^2. **Fig. 3** shows the site location. As shown from the google map, the site is bounded by streets from the four sides. The Available survey of the site showed that the terrain levels ranged from -1.0 m to +5.50 m (natural ground level - NGL). Additionally, the Gate project is a residential and a commercial complex which comprises six basements, ground, Mezzanine floor, nine typical floors and a roof. All basement floors will be constructed on the entire area of the site. The entrance level of the commercial mall at El-Nozha street will be at architectural level -5.50 (i.e. -0.50 NGL).

Fig. 3. Site location (photo from Google map).

3.2 Ground soil investigation and *subsurface* conditions

An extensive ground investigation program was performed in the field and in the laboratory, including more than 60 boreholes with depths of 35m was mechanically drilled throughout the site, as shown in **Fig. 4**, using the rotary drilling technique utilizing bentonite slurry as the drilling fluid. Standard Penetration Test (SPT) and unconfined compression tests have been conducted continuously for sandy and clayey soil layers, respectively, during boring of each borehole. Undisturbed samples were retrieved using the core barrels in rock layers. Additionally, laboratory tests were conducted on the extracted soil sample such as sieve analysis, Atterberg limits, consolidation, direct shear test, unconfined compressive strength tests, etc. **Table 1** summarizes the important soil parameters and physical properties of the main soil layers.

Investigation of the drilled boreholes and examination of the physical and the mechanical properties of the soil indicate that the soil in the site there is a great inhomogeneity. However, four distinct types of soil layers can be found in the site namely: silty sand, shallow clay (clay I), deep clay (clay II), and weak calcareous sandstone. Those layers are located at levels of -2.0, -4.0, -15.60, and -12.0m from the natural ground level and the thickness of each layer extends to 11.0, 9.0, 14.0, and 8.0m, respectively.

No ground water appeared in the boreholes. However due to the site nature being surrounded by many shallow-founded residential buildings and the presence of main utility lines, potential water leakage toward site excavation level is expected. Water levels were only recorded in some boreholes, especially those located along the site perimeter, from depths ranging from 13.50 m to 17.00 m from the ground surface. These levels are mainly leakage from the nearby community. Moreover, regarding the seismic action for the proposed site, the site is located within earthquake zone of “class C” which has a peck ground acceleration of 0.15g (According to the Egyptian code of building loads, 2008).

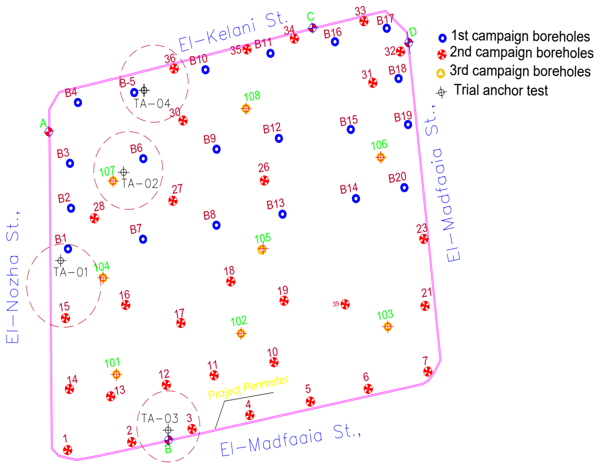

Fig. 4. Locations of the drilled boreholes and the ground anchor tests.

Table 1. Soil parameters and physical properties of the main soil layers found in the site.

Soil type	Silty sand	Shallow clay (Clay I)	Deep clay (Clay II)	Calcareous sandstone
Unit weight γ (kN/m^3)	18	17.9	19	22.5
Young’s modulus E (MPa)	30	37	44	60
Undrained cohesion C_u (MPa)	0.015	0.150	0.20	3
Unconfined compressive strength q_{un} (MPa)	------	------	------	5.1
RQD %	------	------	------	15
N_{SPT}	50	41	50	------
Internal friction angle φ	38	------	------	43
Natural moisture content w_n %	------	42.26	34	------
Atterberg limits L_L, P_L, P_I, and I_c	------	55.6%, 22.7%, 32.9, and 0.41	63%, 30%, 33, and 0.88	------
Compression index C_c	------	0.154	0. 678	------
Fines content %	30	54.5	72.76	------

Note: RQD= Rock quality designations, L_L= liquid limit, P_L= plastic limit, PI= Plasticity index, and I_c= consistency index, where $I_c = \dfrac{L_L - w_n}{L_L - P_L}$.

4. Full-scale anchor tests

4.1 Method of installation of ground anchors

The transfer of shear stress from the fixed anchor to the surrounding soil is also affected by construction technique. The method of installation adopted herein was “type C anchorage” (refer to BS 8081, 1989) because this construction technique is commonly applied in cohessionless soils, and some success has been achieved in stiff cohesive deposits. The following procedures have been used during the installation of ground anchors:

i. Drilling of borehole for anchor was performed by rotary method using bentonite slurry to aid the drilling operation with nominal diameter of 133mm.
ii. After reaching the final level of boring, drilling bentonite shall be flushed out by fresh bentonite and drilling rods shall be withdrawn.
iii. Following the removal of drilling rod, the pre-fabricated anchors were lifted and installed in the borehole.
iv. Cement grout was prepared by mixing potable water with cement (w/c ratio of 0.45 to 0.5). For the purpose of quality control, 6 cubes of the grout mix were taken for compressive strength tests after 7 and 28 days.
v. After the anchor installation, the initial grouting phase was taken place by pumping cement grout (under low pressure) from bottom to top in order to replace the bentonite suspension. Grout filling continued till the cement grout started to come out from borehole (complete filling).
vi. Post-grouting phase was taken place along the bond length at least 24 hours from cement filling (initial grouting phase). Water was pumped under high pressure to fracture the cement cover. After cover fracture, cement grout of mix w/c ratio of 0.45 to 0.5 was pumped in each pipe till reaching injection pressure of about 2000 kPa. If the pressure is not reached after pumping 150 liters of grout per lining tube, grouting was terminated and would be repeated after at least 24 hours to pump till reaching the above pressure or a quantity of 75 liters, whichever is reached first.

Figure 5 shows the values of post-grouting pressures mobilized during the second grouting phase and the corresponding volumes of grout slurry for the four anchors. Volume of the pumped grout can be controlled during post-grouting phase by using an external calibrated pump-piston-pot unit which can control the quantity of the cement grout mixed in the pot, the number of stroke counts done by the piston, and the corresponding measured pressure during pumping.

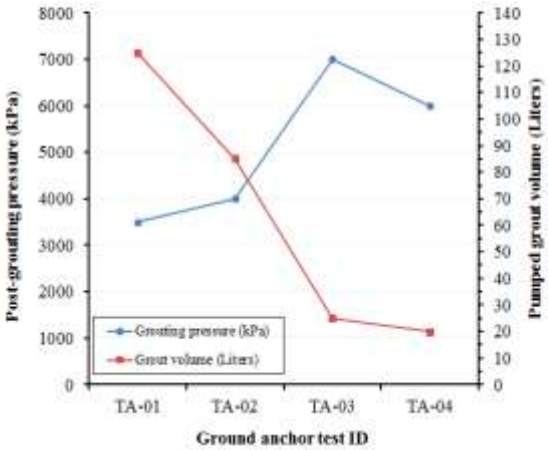

Fig. 5. Post-grouting pressure and the corresponding quantities of pumped grout for all anchors.

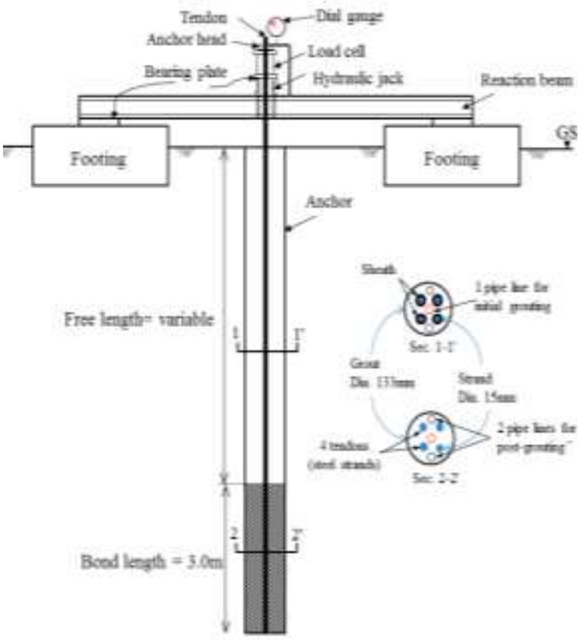

Fig. 6. Schematic of field anchor pull-out test setup.

4.2 Field test setup

Figure 6 illustrates the pullout test setup which includes the load cell, hydraulic jack, dial gauge, etc. Installation of full-scale anchors is required mainly for evaluating the bearing capacity of anchors, demonstration of the behavior and performance of the proposed working anchors, and for proving the quality of the design. Thus, the four anchor tests were carried out at different locations and different soil types. The free length and the bond length of the tested anchors as well as the nearby boreholes are summarized as given in **Table 2**. Short bond length (3m) has been chosen for the all ground anchor tests in order to guarantee that the ultimate pullout failure load can be reached without failure of the tendon, the grout-tendon, or the grout-encapsulation interface.

Moreover, longitudinal soil profiles showing the soil stratification in which the full scale trail anchors were executed are presented in **Figs 7, 8, 9,** and **10**, as well as the elevation of all soil strata based on the nearest boreholes. Those figures also show the locations of the test anchors TA-01, TA-02, TA-03 and TA-04 installed in silty sand, clay I (shallow), clay II (deep), and sandstone, respectively.

Table 2. Data of the full-scale trail anchor tests.

Test ID	Tested soil layer	Anchor total length (m)		Coordinates of test location	Nearest borehole
		L_{free}	L_{fixed}		
TA-01	Clayey silty sand	9	3	E = 1007 N = 1106	B-01 & 15
TA-02	Clay I (Shallow)	6	3	E = 1029 N = 1103	BH-107 & B-06
TA-03	Clay II (Deep)	19	3	E = 1064 N = 1027	BH-B & 3
TA-04	Sand-stone	13	3	E = 1051 N = 1186	B-05 & 36

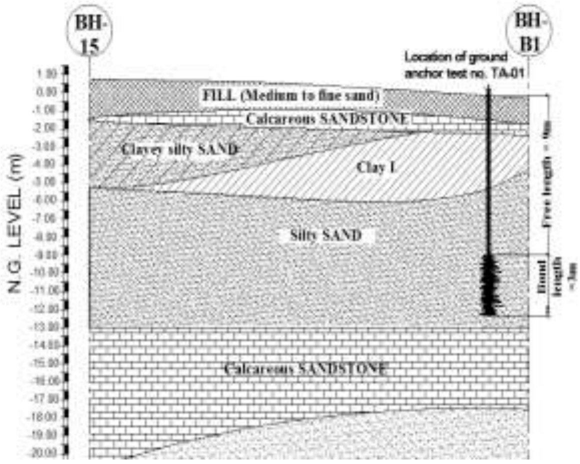

Fig. 7. Soil profile of the test anchor TA-01 based on the nearest borehole.

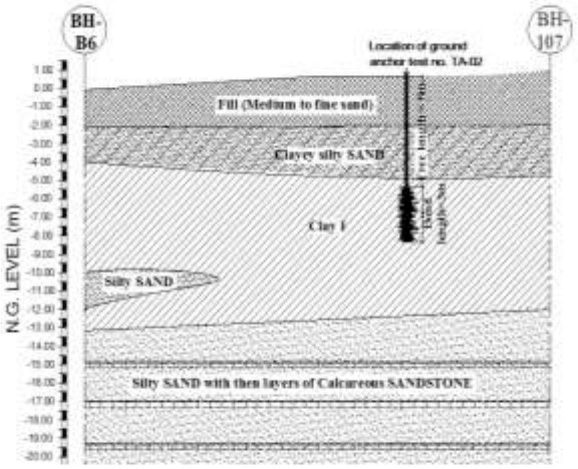

Fig. 8. Soil profile of the test anchor TA-02 based on the nearest boreholes.

Table 3. Load increments and observation periods during the test.

Cycle no.	Test load %	Load (kN)	Time (min)
1	10	70	1
	25	175	1
			2
			3
			5
			10
			15
	10	70	1
2	10	70	1
	25	175	1
	40	280	1
			2
			3
			5
			10
			15
	25	175	1
	10	70	1
3	10	70	1
	40	280	1
	55	385	1
			2
			3
			5
			10
			15
	40	280	1
	10	70	1
4	10	70	1
	55	385	1
	70	490	1
			2
			3
			5
			10
			15
	55	385	1
	10	70	1
5	10	70	1
	70	490	1
	85	595	1
			2
			3
			5
			10
			15
	70	490	1
	10	7	1
6	10	7	1
	85	595	1
	100	700	1
			2
			3
			5
			10
			15
			20
			30
			45
			60
	85	595	1
	10	7	1

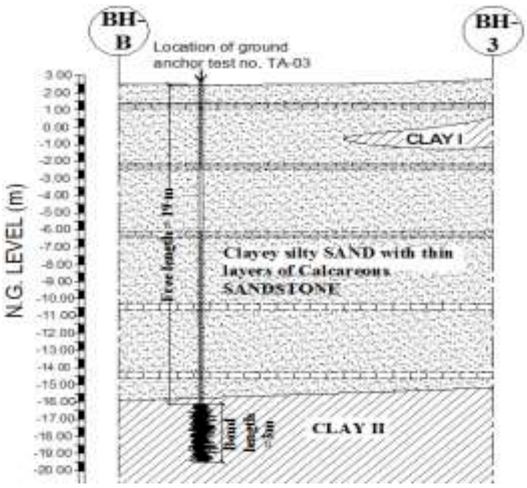

Fig. 9. Soil profile of the test anchor TA-03 based on the nearest boreholes.

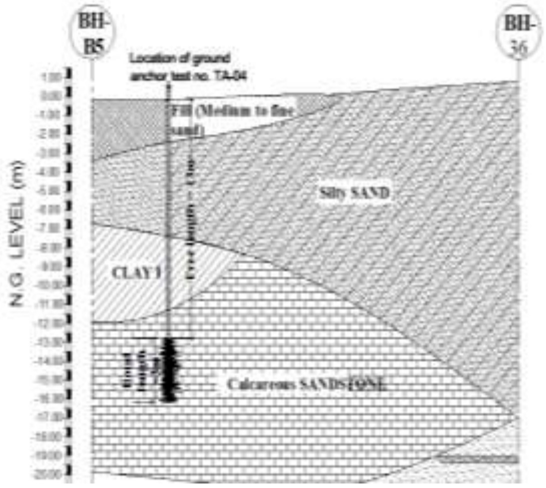

Fig. 10. Soil profile of the test anchor TA-04 based on the nearest boreholes.

4.3 Test load and loading increments

The test protocol and the load increments/decrements rates have been applied as presented in **Table 3**. Typically, 6-cycles of loading, unloading, and re-loading were carried until reaching to the test load of 700kN (70% of the characteristic strength of the tendon). Each loading/unloading stage has been held for at least 1 min, meanwhile the displacement was recorded at the beginning and end of each period. In the intermediate and the peak loading stages this period was extended to for 15 and 60 mins, respectively.

5. Analysis of results

5.1 Load-displacement curves

The results of full-scale pullout tests of the four anchors are shown in **Figs 11, 12, 13,** and **14**. The load-displacement curves for the tests show that only test (TA-04) has achieved the test load and the 6 cycles of loading-reloading have been completed. However, the other three pullout tests (i.e., TA-01, TA-02, and TA-03), the test load cannot reach since an excessive elongation readings have been encountered at cycles 5, 4 and 2, respectively.

It is clear from **Figs 11, 12,** and **13** that failure loads have been obviously reached during pullout tests for ground anchors TA-01, TA-02, and TA-03, which gave failure loads of 515kN, 436kN, and 198kN, respectively. On the other hand, for the fourth ground anchor installed in sandstone (TA-04), the failure load has not been achieved. Therefore, Chin-Kondner method (1970) was used to predict the failure load, as shown in **Fig. 15** the estimated failure load is 1111kN.

Based on those findings, a comparison study was performed between the field tests output and the corresponding design values recommended by the well-known codes of practice (AASHTO, 2004; BS 8081, 1989; and CFEM, 2006) for estimating of ultimate unit skin friction resistance for ground anchors in soil and rock layers (grout-soil interface). Furthermore, **Table 4** presents the failure pullout tests results and the ultimate unit skin friction resistance for all ground anchor tests.

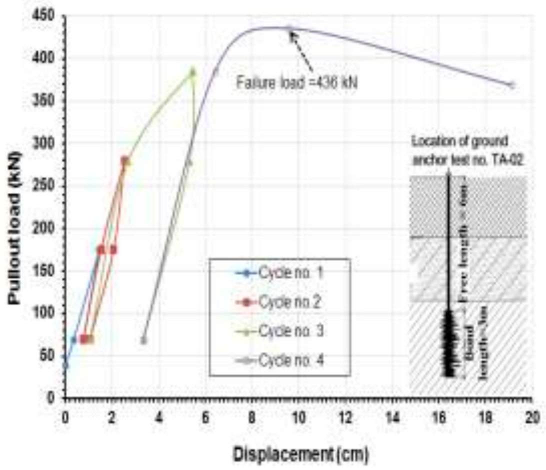

Fig. 12. Pullout load-displacement curve for ground anchor TA-02 installed in shallow clay (clay I) soil.

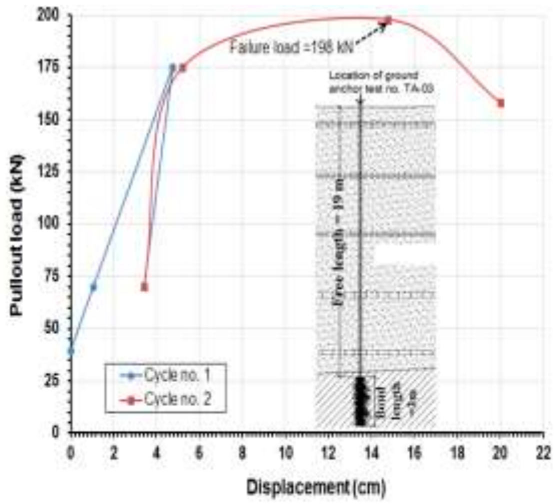

Fig. 13. Pullout load-displacement curve for ground anchor TA-03 installed in deep clay (clay II) soil.

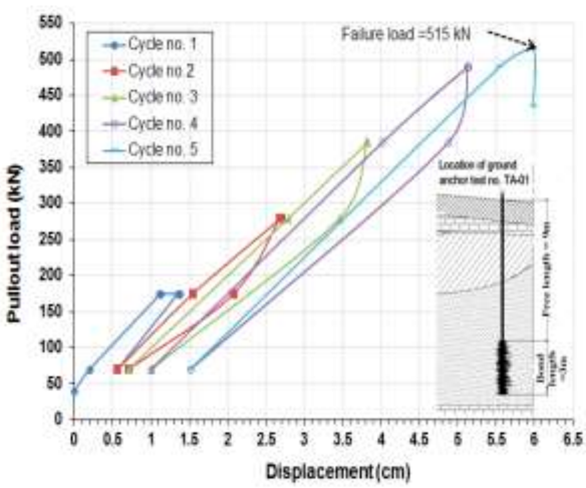

Fig. 11. Pullout load-displacement curve for ground anchor TA-01 installed in silty sand soil.

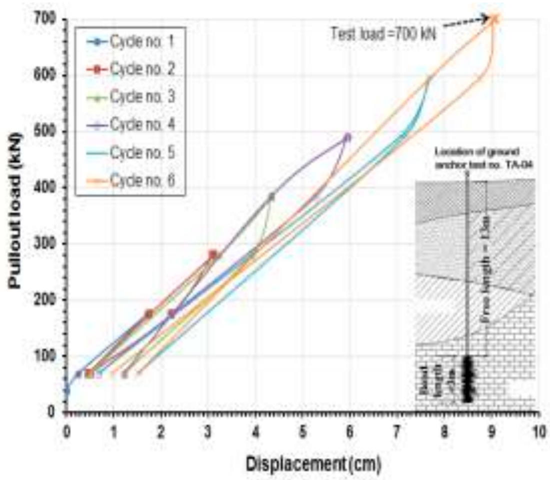

Fig. 14. Pullout load-displacement curve for ground anchor TA-04 installed in sandstone.

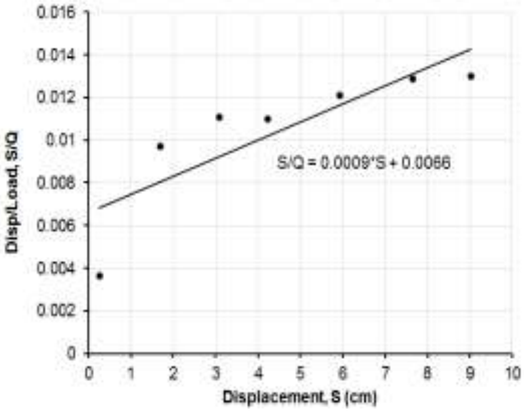

Fig. 15. Pullout load-displacement curve for ground anchor TA-04 installed in sandstone.

Table 4. Failure loads obtained from the full-scale anchor tests and corresponding ultimate unit skin friction resistance for each soil type.

Test ID	Tested soil layer	Bond length (m)	Ultimate/ failure pullout load, Q_{ult} (kN)	Ultimate unit skin friction per unit length (kN/m)
TA-01	Silty sand	3	515	171.7
TA-02	Shallow clay (Clay I)	3	436	145.3
TA-03	Deep clay (Clay II)	3	198	66
TA-04	Sandstone	3	1111	370.4

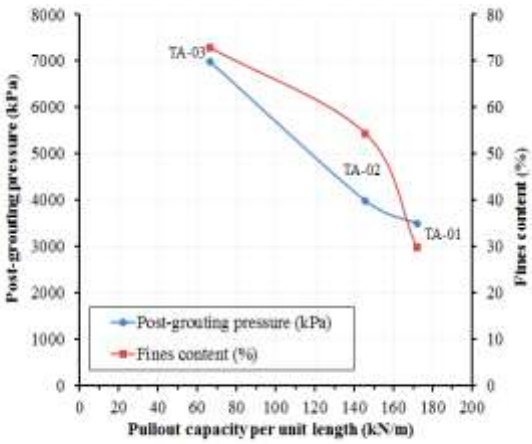

Fig. 16. Effect of the fines content and post-grouting pressure on the pullout capacities of ground anchors.

5.2 Influence of the fines content and grouting pressure on the pullout capacity

Figure 16 shows the effect of fines content of the soil layers in which the fixed length of the ground anchors were installed on the pullout capacities of the anchors. It is clear that the fines content of the soils have a significant impact on the pullout capacity where the pullout failure loads increase when the fines content of the soil layer decrease. For silty sand soil layer, which has fine content of 30%, gives pullout failure load of 515kN. For shallow clay layer, which has fine contents of 54.5%, gives pullout failure load of 436kN. For deep clay layer, which has fine contents of 72.8%, gives pullout failure load of 198kN.

In addition, post-grouting pressure has influence on the pullout failure loads of the anchors. As can be noticed in Fig. 16 that by increasing the content of fine particles in the soil around the fixed length of the anchor that causes rising in grouting pressure during post-grouting phase which in turns results in reduction of failure pullout loads of the anchor. This may be owned to that the presence of high percentage of fine particles in soil structure near to the vicinity of fixed length of an anchor, leads to clogging of grouting slurry being entered between soil particles. Consequently, improvement in grout-soil interface shear strength properties (i.e., unit skin friction resistance) would not occur.

5.3 Comparative study

A comparison study was conducted between the field test results and the estimated values of skin friction resistance given in the codes of practices used in this work. **Table 5** represents the summary of the obtained results from field tests along with the corresponding design values recommended by the codes of practice.

Figure 17 illustrates the measured field skin friction and the corresponding design values given in the code of practice. By comparing the measured field skin friction results against the values recommended by the codes of practice used in this study, it can be seen that AASHTO (2004) and BS 8081 (1989) reveal the most reasonable and satisfactory results over the other codes of practice. For ground anchor tests (AT-01 and AT-04) installed in silty sand and calcareous sandstone, their measured field unit skin frictions are 171.7 and 370.4 kN/m, respectively, while AASHTO (2004) yields unit skin friction values of 167 and 334 kN/m for anchors installed in silty sand and calcareous sandstone, respectively. Comparing those values to the actual field results, it can be implied that AASHTO (2004) gives an excellent prediction for the pullout forces for the ground anchors constructed in silty sand, and calcareous sandstone. Besides, BS 8081 (1989) shows a good predictability for the anchors installed in shallow clay and calcareous sandstone, however, BS 8081 (1989) shows high prediction to the unit skin friction for the anchors installed in silty sand and deep clay soils.

Table 5. Summary of the field tests results and design values recommended by the widely used codes of practice.

Test ID	Tested soil layer	Ultimate unit skin friction per unit length (kN/m)						
		Field results	AASHTO (2004)	Variation %	BS 8081 (1989)	Variation %	CFEM (2006)	Variation %
TA-01	Silty sand	171.7	167	2.74	217.2	27.25	130	19.20
TA-02	Shallow clay (Clay I)	145.3	92	36.68	103.1	45.54	60	82.50
TA-03	Deep clay (Clay II)	66	146.2	121.52	129.5	43.43	60	4.63
TA-04	Calcareous sandstone	370.4	334	9.83	355	4.61	430	16.79

Note: Variation%= (field results-predicted results)*100/field results

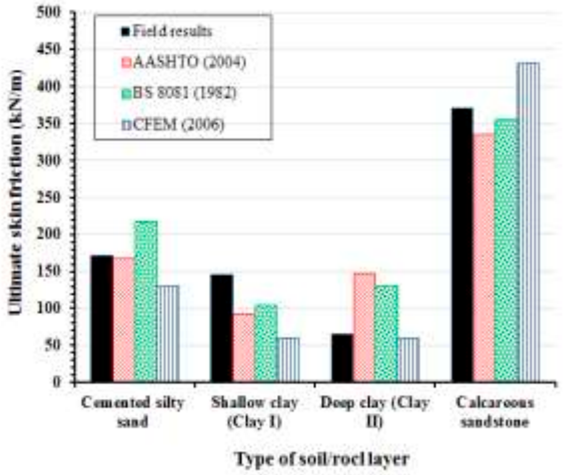

Fig. 17. Variation of unit skin friction per unit length of ground anchors for field tests and the codes of practice.

On the other hand, it is noticeable that the CFEM (2006) displays the lowest predictability among all codes of practice, except for test TA-04 (sandstone). This can be attributed to that the Canadian Foundation Engineering Manual (2006) introduces unit skin friction design values for only single stage grouted anchors, however two stage grouted anchors were used in this study. Generally, multiple stages of grouting increase the values of skin friction at bond length of anchor because of compaction of the surrounding ground.

Consequently, the pullout capacity of ground anchor does not only depends on the stiffness of the soil layer in which its bond length is installed, but also on other major parameters that are related to particle size distribution (i.e., fines content percent) and method of installation (i.e., post-grouting).

It is important to mention that those full-scale tests used in this study do not cover all types of the Egyptian soil formations, therefore extra numerous full-scale anchors are needed in order to introduce the Egyptian guidelines for design and construction of ground anchors based on local experience.

6. Summary and conclusion

Four full-scale pullout tests of ground anchors were performed into four different types of soil deposits in Egypt, namely silty sand, clay I (shallow), clay II (deep), and sandstone. Furthermore, an extensive ground investigation campaign was performed at the site location to determine the physical and mechanical properties of the soil layers in which the ground anchors were installed. Field test setup and installation method of the ground anchors were explained. The results of the field tests were compared against the design values of unit skin friction resistance given by the well-known codes of practice. The main findings can be summarized as follow:

1. Fine contents of soil layer, in which the fixed length of the ground anchor is installed, plays significant role in the pullout capacity of an anchor as the pullout capacity increases when the fines content of the soil layer decreases.
2. For ground anchors installed into silty sand soils and weathered rock formations, post-grouting has a noticeable effect on the values of skin friction resistance. Second grouting phase under pressure greater than 2000 kPa results in increasing of grout-soil/rock interface shear strength adjacent to bond length of the anchor.
3. Pullout capacities of ground anchors not only depend on the soil stiffness in which their bond lengths are installed, but also on other major parameters than are related to particle size distribution of the soil layers (i.e., fines content percent) and method of installation of anchors (i.e., post-grouting).
4. The AASHTO (2004) and the BS 8081 (1989) codes of practice revealed the most reasonable and satisfactory results over the CFEM (2006) when they are compared to the actual field results. It is obvious that AASHTO (2004) gives an excellent prediction for the pullout forces for the ground

anchors constructed in silty sand and calcareous sandstone. Besides, BS 8081 (1989) shows a good predictability for the anchors installed in shallow clay and calcareous sandstone, however, BS 8081 (1989) over-predicts the pullout capacities for the anchors installed in silty sand and deep clay soils. This indicates that the values of skin friction resistance between anchor and soil/rock interface recommended by AASHTO (2004) and BS 8081 (1989) can be adopted for determination of pullout capacities of ground anchors installed in Egyptian soils.

Appendix (A)

This appendix summarizes the design tables and charts given by each code of practice used in the paper (AASHTO, BS 8081, and FHWA) for prediction of ultimate skin friction resistances (τult).

A.1 Estimation of pullout anchor capacity using AASHTO (2004)

Tables A-1, A-2, and A-3 represent the presumptive values that may be used to estimate the nominal (ultimate bond for small diameter anchors installed in cohesive soils, cohesionless soils, and rock, respectively.

A.2 Estimation of pullout anchor capacity using BS 8081 (1989)

Figs A-1 and A-2 give the relationships between the fixed length and the ultimate skin friction resistance recommended by the BS 8081 (1989) for cohesionless and cohesive soils, respectively. Those design charts are based on previous field work on ground anchor tests done by Ostermayer and Scheeie (1978) and Ostermayer (1974).

For anchors in rock, BS 8081 (1989) provides guide design values of rock-grout bond stress as shown in **Table A-4**.

A.3 Estimation of pullout anchor capacity using CFEM (2006)

Canadian Foundation Engineering Manual (2006) introduces the design values given in **Tables A-5 and A-6** for estimation of ultimate skin friction resistance per unit length of bond length for ground anchors installed in rock.

Table A-1. Presumptive ultimate unit skin friction stress for anchors in cohesive soils (AASHTO, 2004).

Anchor/soil type (grout pressure)	Soil stiffness (q_{un}, MPa)	Presumptive ultimate unit skin friction stress, τ_{ult} (kPa)
Gravity grouted anchors (<350kPa) Silty-clay (mixtures)	Stiff to very stiff 0.096-0.383	30 - 70
Pressure grouted anchors (350-2800kPa)		
High plasticity clay	Stiff 0.096-0.239 Very stiff 0.239-0.383	30 - 100 70 – 170
Medium plasticity clay	Stiff 0.096-0.239 Very stiff 0.239-0.383	100 - 250 140 - 350
Medium plasticity sandy silt	Very stiff 0.239-0.383	280 - 380

Table A-2. Presumptive ultimate unit skin friction stress for anchors in cohesionless soils (AASHTO, 2004).

Anchor/soil type (grout pressure)	Soil compactness or N_{SPT}	Presumptive ultimate unit skin friction stress, τ_{ult} (kPa)
Gravity grouted anchors (<350kPa) Sand or sand-gravel mixtures	Medium dense to dense 11-50	70 - 140
Pressure grouted anchors (350-2800kPa)		
Fine to medium sand	Medium dense to dense 11-50	80 - 380
Medium to coarse sand with gravel	Medium dense 11-30 Dense to very dense 30-50	110 - 670 250 - 950
Silty sand	----------	170 - 400
Sandy gravel	Medium dense to dense 11-40 Dense to very dense 40-50	210 - 140 280 - 1400
Glacial till	Dense 31-50	300 - 520

Table A-3. Presumptive ultimate unit skin friction stress for anchors in rock (AASHTO, 2004).

Rock type	Presumptive ultimate unit skin friction stress, τ_{ult} (kPa)
Granite to Basalt	1700 - 3100
Dolomite limestone	1400 - 2100
Soft limestone	1000 - 1400
Slates and hard shales	800 - 1400
Sandstones	800 - 1700
Weathered sandstones	700 - 800
Soft shales	200 - 800

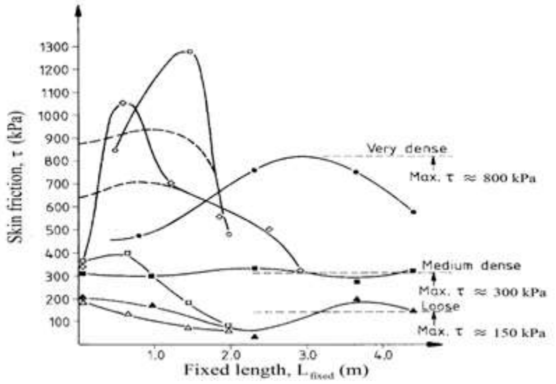

Fig. A-1. Distribution of long-term skin friction (f) at ultimate load in relation to anchor bond length and soil density (after Ostermayer and Scheeie, 1978)

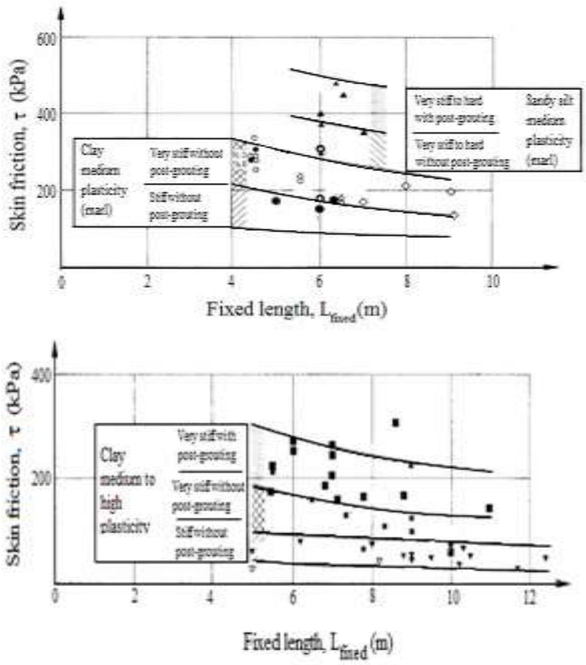

Fig. A-2 Skin friction (f) in cohesive soils for various bond lengths, with and without post-grouting (after Ostermayer, 1974).

Table A-4. Rock-grout bond values for design recommended by BS 8081, 1989 (after Littlejohm and Bruce, 1977).

Rock type	Working bond	Ultimate bond	Load factor of safety
Weathered sandstone	-------	0.69 - 0.85	3
Bunter sandstone	0.4	-------	3
Bunter sandstone (ultimate compressive stress>2.0Mpa)	0.6	-------	3
Hard fine sandstone	0.69 - 0.83	2.24	2.7 - 3.3
Sandstone	-------	0.83 - 1.73	1.5 - 2.5
Weak rock	0.35 - 0.70	-------	-------
Medium rock	0.70 - 1.05	-------	-------
Strong rock	1.05 - 1.4	-------	-------

Table A-5. Estimation of grout-soil resistance per unit length for pressure-grounded anchors (CFEM, 2006).

Ground type	Relative density/consistency (N_{SPT} range)	Ultimate skin friction per unit length (kN/m)
Sand and gravel	Loose (4 – 10)	145
	Medium compacted (10 – 30)	220
	Compacted (30 – 50)	290
Sand	Loose (4 – 10)	100
	Medium compacted (10 – 30)	145
	Compacted (30 – 50)	190
Sand and silt	Loose (4 – 10)	70
	Medium compacted (10 – 30)	100
	Compacted (30 – 50)	130
Low-plasticity silt and clay	Stiff (10 - 20)	30
	Hard (20 - 40)	60

Table A-6. Estimation of grout-soil resistance per unit length for pressure-grounded anchors in rock (CFEM, 2006).

Rock type	Ultimate skin friction per unit length (kN/m)
Granite or Basal	730
Dolomitic limestone	580
Soft limestone	430
Sandstone	430
Slates and hard shales	360
Soft shales	145

References

American Association of State Highway and Transportation Officials (AASHTO), 2004. LRFD Bridge Design Specification, SI units, Second Edition.

Barley, A.D., 1997a. The single bore multiple anchor system. Proc. of the conference on ground anchorages and anchored structures, Institution of Civil Engineers, 20-21 March, 1997, London: 65-75.

Barley, A.D., 1997b. Properties of anchor grout in a confined state. Proc. of the conference on ground anchorages and anchored structures, Institution of Civil Engineers, 20-21 March, 1997, London: 13-22.

Benmokrane, B., Chekired, M. and Xu, H., 1995. Monitoring behavior of grouted anchors using vibrating-wire gauges. Journal of Geotechnical Engrng, ASCE, **121** (6):466–75.

Briaud, J.L., Powers W.F. and Weatherby, D.E., 1998. Should grouted anchors have short tendon bond length? Journal of Geotechnical and Geoenvironmental Engrng., ASCE, **124** (2):110–119.

British Standard Code of practice for Ground Anchorages (BS 8081). 1989.

The European Standard EN 1537, 1999. Execution of special geotechnical work of ground anchors. http://geotechnicaldesign.info/en1537-1999.html

Canadian Foundation Engineering Manual, 2006. Fourth Edition, Canadian Geotechnical Society.

Cheney, R.S., 1984. Permanent ground anchors. FHWA-DP-68-IR Demonstration Project. Federal Highway Administration, U.S. Department of Transportation, Washington, DC: pp 132.

Chin, F. K., 1970. Estimation of the ultimate load of piles from tests not carried to failure. Proc. of the 2nd South-East Asian Conference on Soil Eng., Singapore: 81-90.

Egyptian code of practice for soil mechanics and foundation design and construction, 2005. Cairo, Egypt.

Egyptian code of practice for building loads and structural forces, 2008. Cairo, Egypt: pp. 115.

Jarrel, D.J., 1997. The Tendon/grout Interface Performance of Grouted Threaded Bar Ground Anchors. Monash University. Dept. of Civil Engineering, Monash University, 1997.

Kim, N.K., 2003. Performance of tension and compression anchors in weathered soil. Journal of Geotechnical and Geoenvironmental Engrng., ASCE, **129** (12): 1138–1150.

Littlejohn, G.S. and Bruce, D.A., 1979. Long term performance of high capacity rock anchors at Devon-port. Ground Engineering, **12** (7): 28-33.

Ostermayer, H., 1974. Construction, caring behavior and creep characteristics of ground anchors. I.C.E. Conference on Diaphragm Walls and Anchorages, London: 141-151.

Ostermayer, H. and Scheele, F., 1978. Research and ground anchors in non-cohesive soils. Revue Française de Geotechnique No.3: 92-97.

Petrasovits, G., 1981. Interaction between soil and ground anchor. Proc. of the International Conference on Soil Mechanics and Foundation Engng., Stockholm: 213-217.

PTI Manual., 1996. Recommendations for pre-stressed rock and soil anchors. Post Tensioning Institute, Phoenix.

Sabatini, P.J., Pass, D.G. and Bachus, R.C., 1999. Ground anchors and anchored system. Geotechnical Engineering Circular No. 4, Report No. FHWA-SA-99-015. Federal Highway Administration, U.S. Department of Transportation, Washington, DC, p. 218.

Weathersby, D.E., 1982. Tieback. FHWA RD-82-047. Federal Highway Administration, U.S. Department of Transportation, Washington, DC: pp 249.

Weerasinghe, R.B. and Littlejohn, G.S., 1977. Load transfer and failure of anchorages in weak mudstone. Proc. of the conference on ground anchorages and anchored structures, Institution of Civil Engineers, London: 33-44.

Woods, R.I., Barkhordari, K., 1997. The influence of bond stress distribution on ground anchor design. Proc. of the conference on ground anchorages and anchored structures, Institution of Civil Engineers, 20-21 March, 1997, London: 55-64.

Symbols and abbreviations

A_g	Grout area
A_s	Cross-sectional area of strand
C_c	Compression index
C_u	Undrained cohesion
C_1	Slope of the straight line
C_2	Intercept of the S/Q axis
D	Diameter of anchor or effective diameter of borehole
d_e	Effective diameter of strand
E	Young’s modulus
f_{ub}	Ultimate bond stress between grout and strand
f_{uc}	Ultimate compressive strength of grout or pure shear strength of grout
f_{us}	Ultimate tensile stress of strand
g	Ground acceleration (9.81 cm/s^2)
I_c	Consistency index
L_e	External length of tendon
L_{fixed}	Fixed/bond length of anchor
L_{free}	Free anchor length
L_L	Liquid limit
L_{tb}	Bonded length of strand
L_{tf}	Tendon free length
n	Number of strands
NGL	Natural ground level
N_{SPT}	Number of bellows of standard penetration test
PI	Plasticity index
P_L	Plastic limit
Q_{uf}	Ultimate friction load
Q_{ug}	Ultimate compressive or shear resistance of grout
Q_{up}	Pullout load capacity
Q_{us}	Ultimate tensile load of strand
q_{un}	Unconfined compressive strength
RQD	Rock quality designations
S	Settlement
w_n	Natural moisture content
φ	Internal friction angle
γ	Unit weight of soil
τ_{ult}	Ultimate skin friction resistance